ULTRA-COMPACT X-RAY BINARIES: DUAL-LINE SOURCES

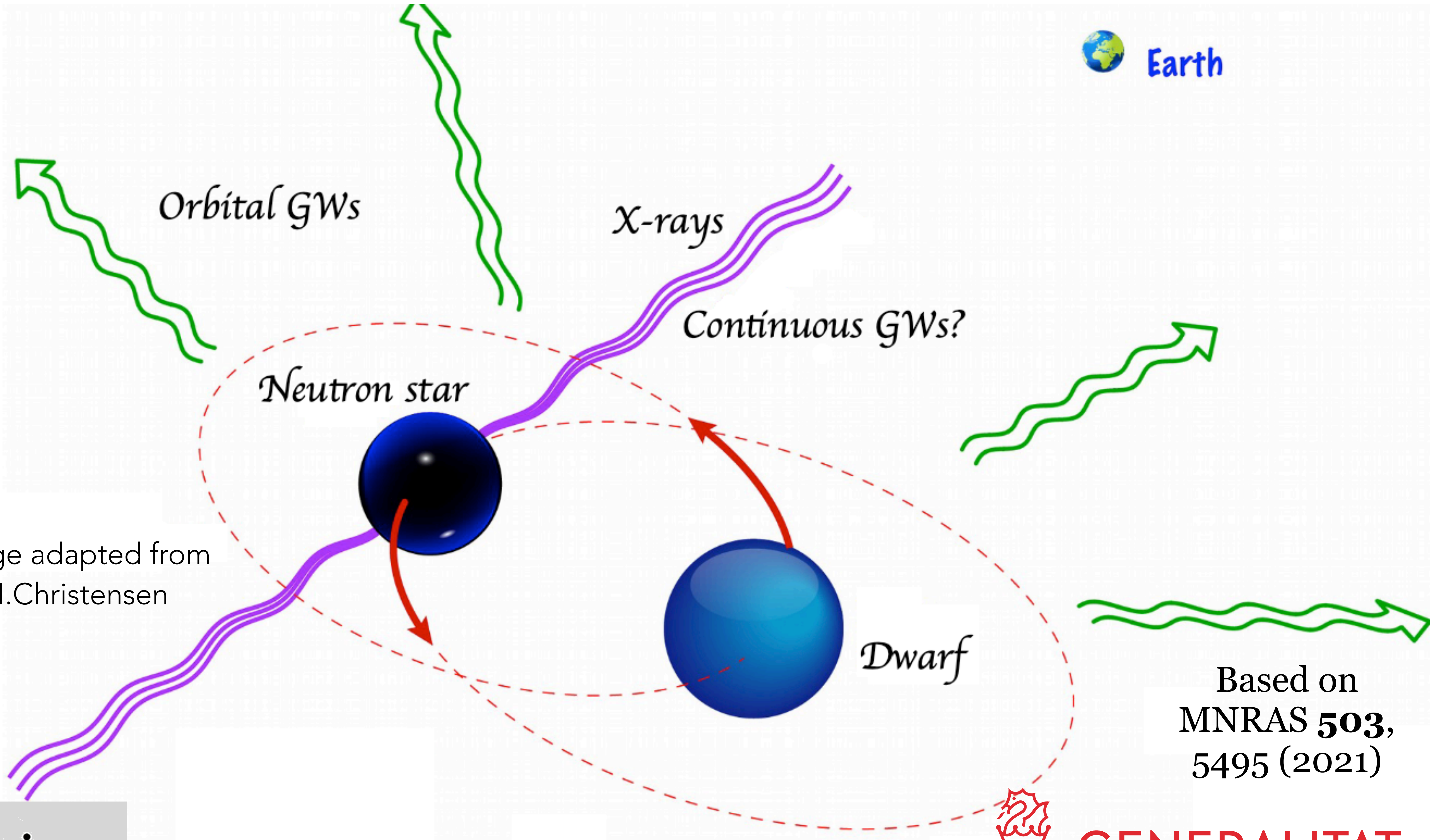

Image adapted from
N.Christensen

Based on
MNRAS **503**,
5495 (2021)

LISA Spain Meeting 2024, October 15

Institute of Space Sciences (ICE, CSIC and IEEC)

Arthur Suvorov

GENERALITAT VALENCIANA
Conselleria de Educación, Cultura,
Universidades y Empleo

WHAT ARE THESE SYSTEMS?

- Ultra-compact X-ray binaries are binaries with orbital periods < 1 hr. They involve a compact object (NS,BH) and a low-mass (<< solar mass) companion

- They arise as the (possibly detached) end state of low-mass X-ray binaries, that have gradually compactified through orbital angular-momentum losses due to a combination of magnetic braking (or other persistent outflows), gravitational-wave emission, and mass transfers; see, e.g., **Chen & Podsiadlowski 2016**

- Companion mass is gradually stripped away, leaving behind a non-degenerate He star or a O/Ne/Mg, C/O, or He white dwarf

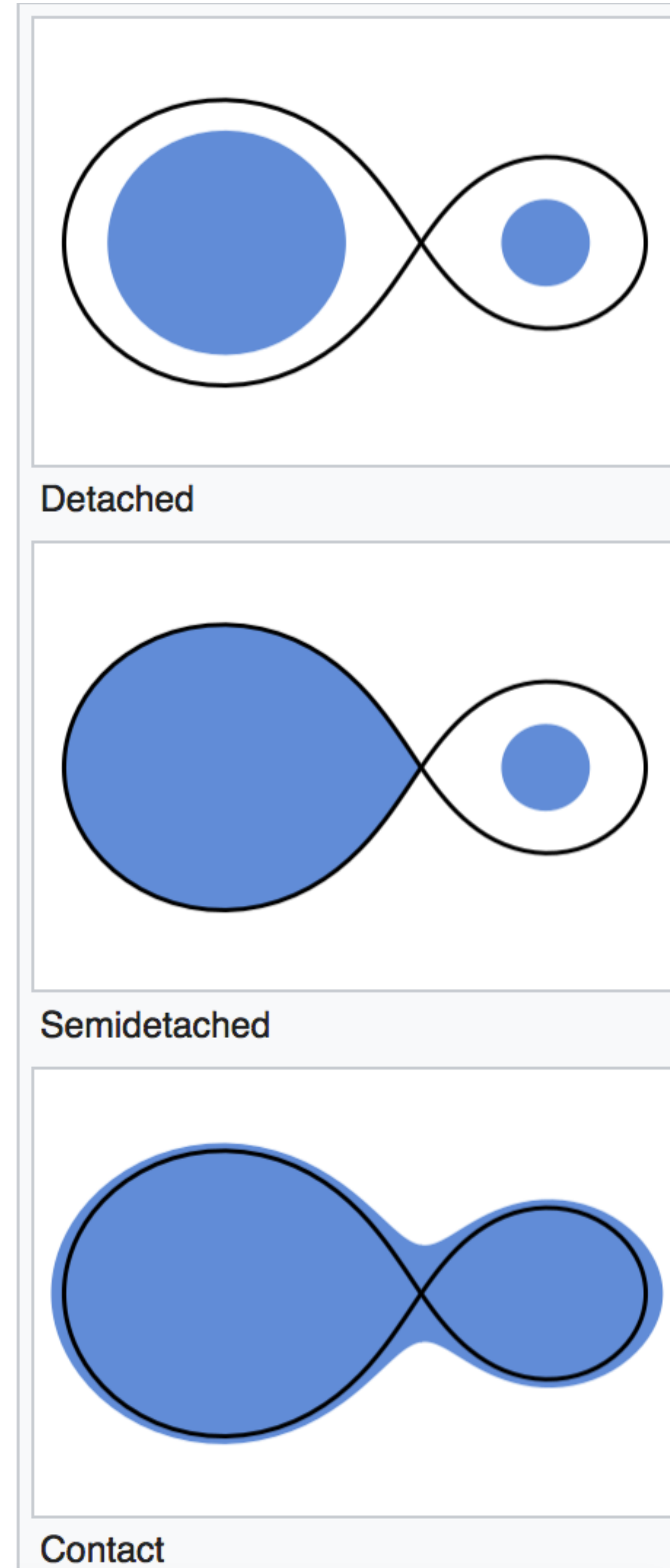

Wiki commons

PRIME TARGETS FOR LISA!

- A circular binary will, in general, emit "orbital" gravitational waves which reduce the angular momentum of the system and shrink the orbit.
- The system radiates at twice the orbital frequency; for UCXBs, this lies in the ~mHz range (e.g. **Thorne 1980**).
- These are almost certainly detectable by LISA!

$$\rho = \delta(z)\left[m_1\delta(x-x_1)\delta(y-y_1) + m_2\delta(x-x_2)\delta(y-y_2)\right]$$

$$\begin{aligned}
I^{xx} &= \int d^3x\,(\rho x^2) = m_1 x_1^2 + m_2 x_2^2 \\
&= \left(\frac{\mu^2 a^2}{m_1^2} m_1 + \frac{\mu^2 a^2}{m_2^2} m_2\right)\cos^2(\omega t) \\
&= \mu^2 a^2 \left(\frac{1}{m_1} + \frac{1}{m_2}\right)\cos^2(\omega t) \\
&= \mu a^2 \cos^2(\omega t) \\
&= \frac{1}{2}\mu a^2 \left(1 + \cos(2\omega t)\right)
\end{aligned}$$

$$\frac{dE_{gw}}{dt} = \frac{G}{c^5}\frac{1}{5}\langle \dddot{\mathcal{I}}_{jk} \dddot{\mathcal{I}}^{jk} \rangle$$

$$h_c \approx 1.9 \times 10^{-20} \left(\frac{1\ \mathrm{hr}}{P_{\mathrm{orb}}}\right)^{7/6} \left(\frac{\mathcal{M}}{1 M_\odot}\right)^{5/3} \left(\frac{10\ \mathrm{kpc}}{d}\right) \qquad \mathcal{M} = \frac{(M_\star M_{\mathrm{comp}})^{3/5}}{(M_\star + M_{\mathrm{comp}})^{1/5}}$$

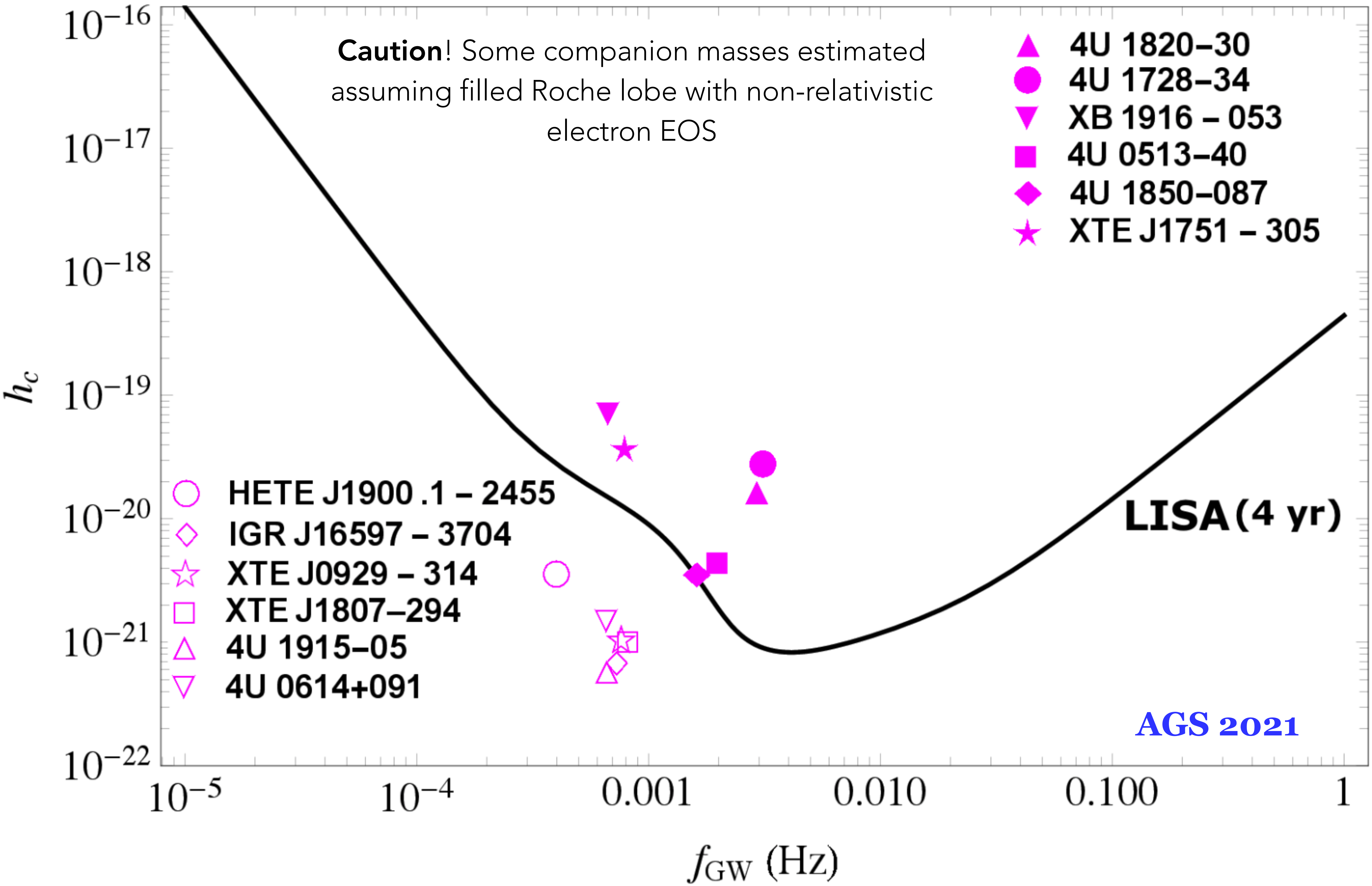

SO WHAT?

- An interesting aspect to these UCXBs is that they sometimes contain a neutron star primary which is rapidly rotating.
- The high X-ray luminosities of most systems also tends to suggest the accretion rate is high, and therefore a significant spin-up torque
- But there is an observational puzzle: NS binaries have a capped spin frequency of around ~700Hz, a factor ≳2 lower than the break-up limit, which you would expect if spun-up indefinitely; **Patruno et al. 2017**
- So *something* is triggering an excess of spin-down; "centrifugal barrier"?

Data compiled AGS 2021

Source	ν_{spin} (Hz)
4U 1820-30[a]	275[#]
IGR J16597-3704[b]	105.2[*]
4U 1728-34[c]	363[†,#]
HETE J1900.1-2455[d]	377.3[*]
XB 1916-053[e]	270[†]
XTE J1807-294[f]	190.6[*]
4U 1915-05[g]	366[#]
4U 0614+091[h]	477[†]
4U 0513-40[i]	($\gtrsim$ 398)
4U 1850-087[j]	(403)
XTE J1751-305[k]	435.3[*]
XTE J0929-314[l]	185.1[*]

X-RAY ACCRETION MODES

- Depending on the relationship between the accretion rate (i.e., X-ray luminosity), the spin of the neutron star and its magnetic field strength, the mode of accretion could be either:

- (a) boundary layer accreted; (b) pole-channeled, or (c) propeller.

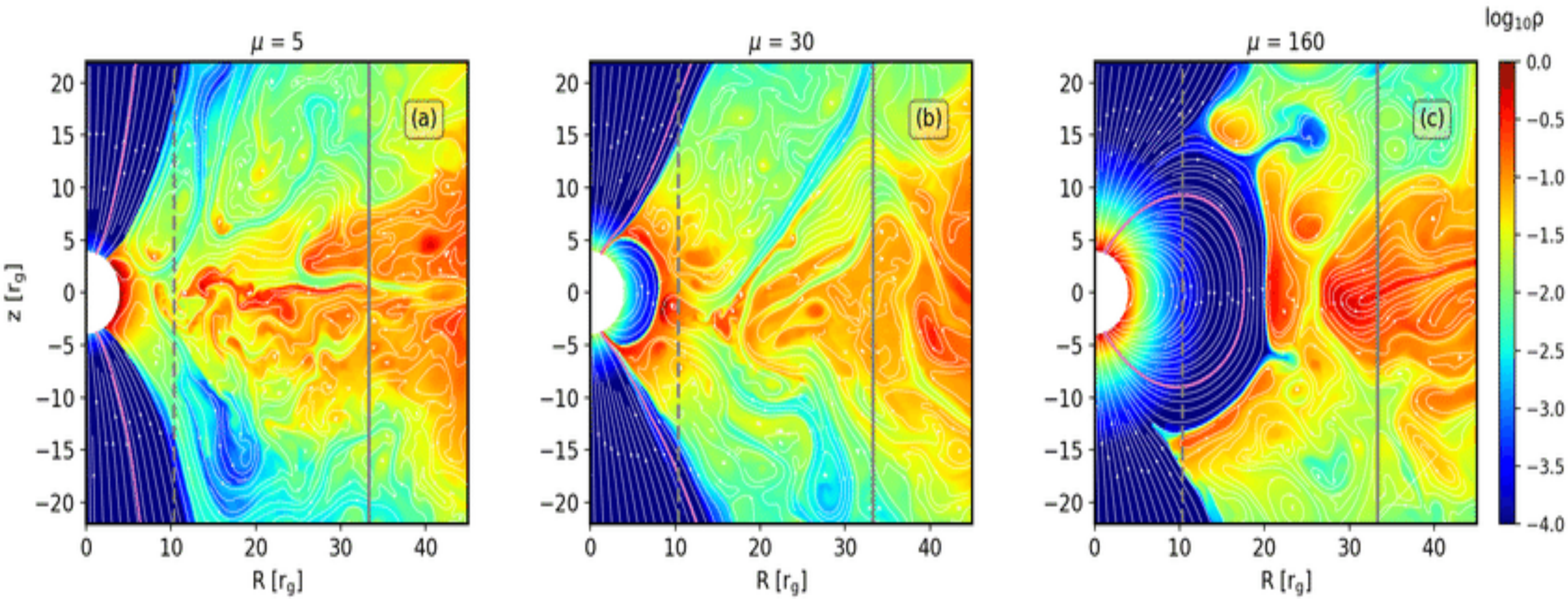

Das et al. (2022)

Matter is force-stopped at the magnetospheric boundary, but if Rco < Rm, the rotating magnetosphere will 'propeller' plasma back beyond the capture radius (Illarionov & Sunyaev 1975)

$$\frac{R_{\rm A}}{R_{\rm co}} \approx 289\,\xi\,\frac{R_6^{12/7} B_{14}^{4/7}}{M_{1.4}^{10/21}\dot{M}_{-10}^{2/7}P_{-1}^{2/3}}$$

PILING IT ON

$$\dot{\nu} \approx 1.4 \times 10^{-13} \left(\frac{10^{45}\ \mathrm{g\ cm^2}}{I_0}\right) \left[\left(\frac{L_X}{10^{37}\ \mathrm{erg\ s^{-1}}}\right)^{6/7} \times \left(\frac{B_\star}{10^8\ \mathrm{G}}\right)^{2/7} \left(\frac{R_\star}{10^6\ \mathrm{cm}}\right)^{12/7} \left(\frac{1.6\mathrm{M}_\odot}{M_\star}\right)^{3/7} - 106 \left(\frac{Q_{22}^{\max}}{10^{38}\ \mathrm{g\ cm^2}}\right)^2 \left(\frac{\nu_{\rm spin}}{500\ \mathrm{Hz}}\right)^5 \right] \mathrm{Hz\ s^{-1}},$$

- Suggested already in the early 90s that gravitational-wave induced spindown may also play a role in limiting the spin frequency; especially this makes sense in the context that the observed values are *capped* at ~700 Hz.

- Other aspects of accretion also: magnetic field may be buried, and a mountain may accrue atop the star.

- Bursts with low recurrence times especially indicative of a mountain or at least "fenced-off" patches of fuel; **Bhattacharyya & Strohmayer 2006**

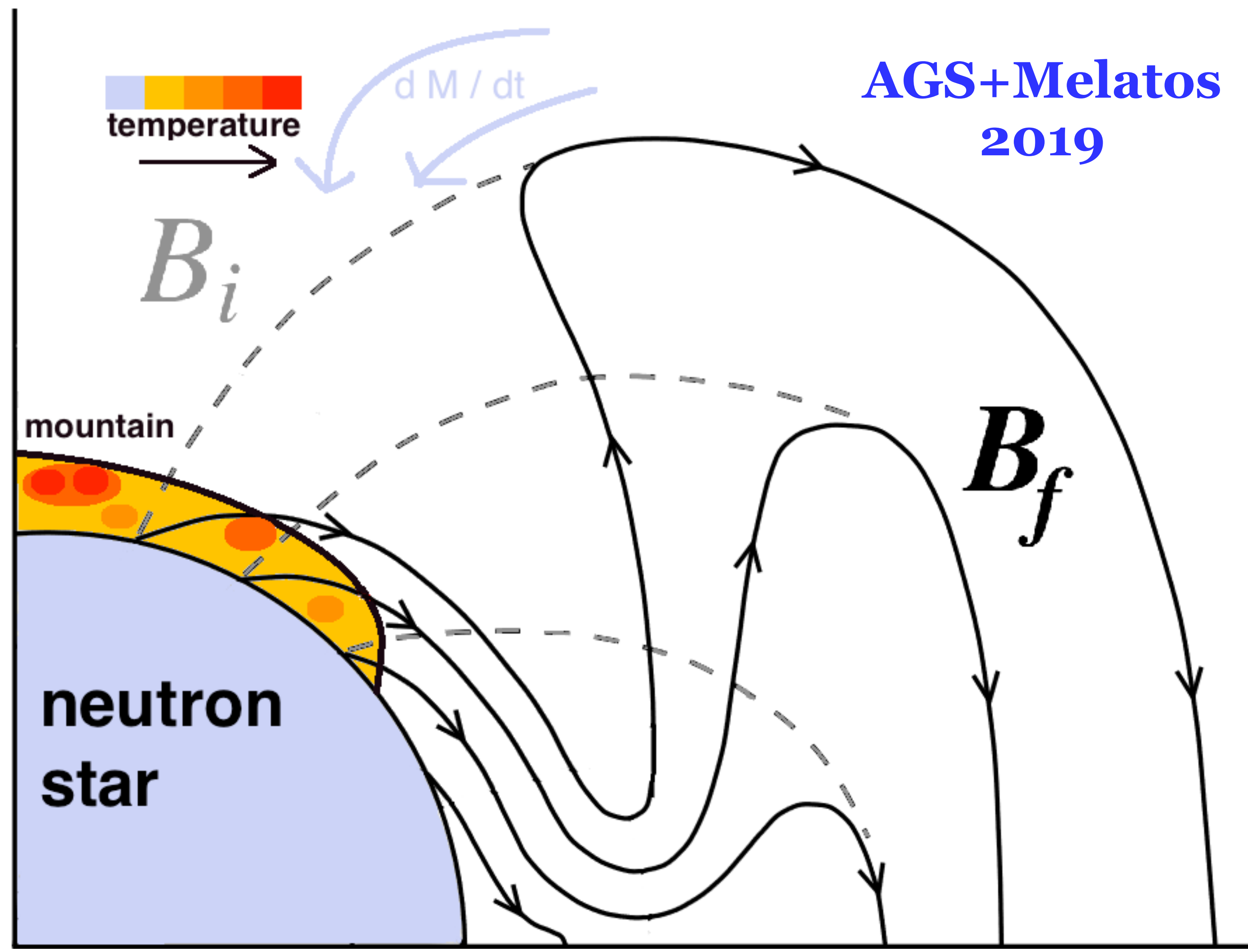

HIDDEN FIELDS?

- Hidden components of the field with large gradients could also produce sizeable GWs!

AGS+Glampedakis 2023

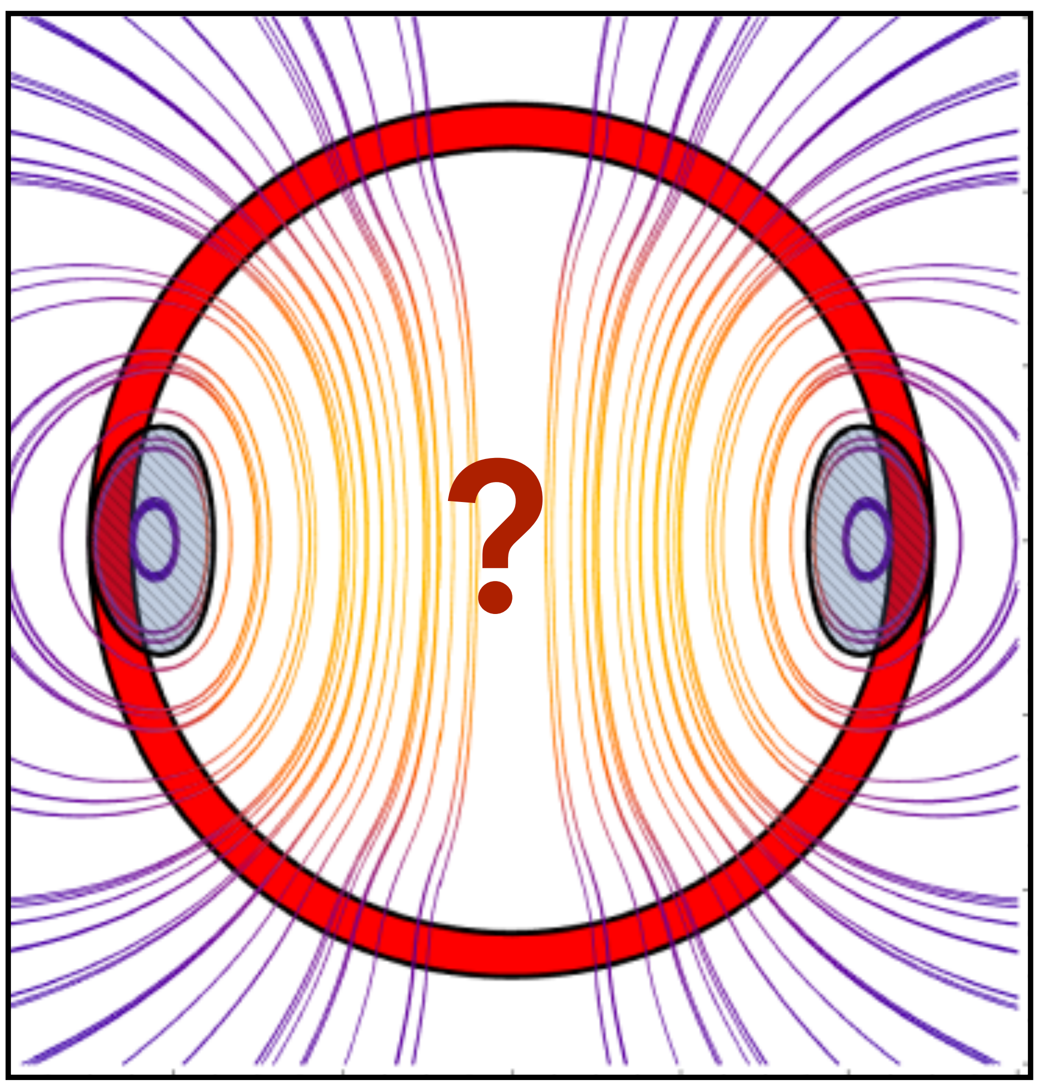

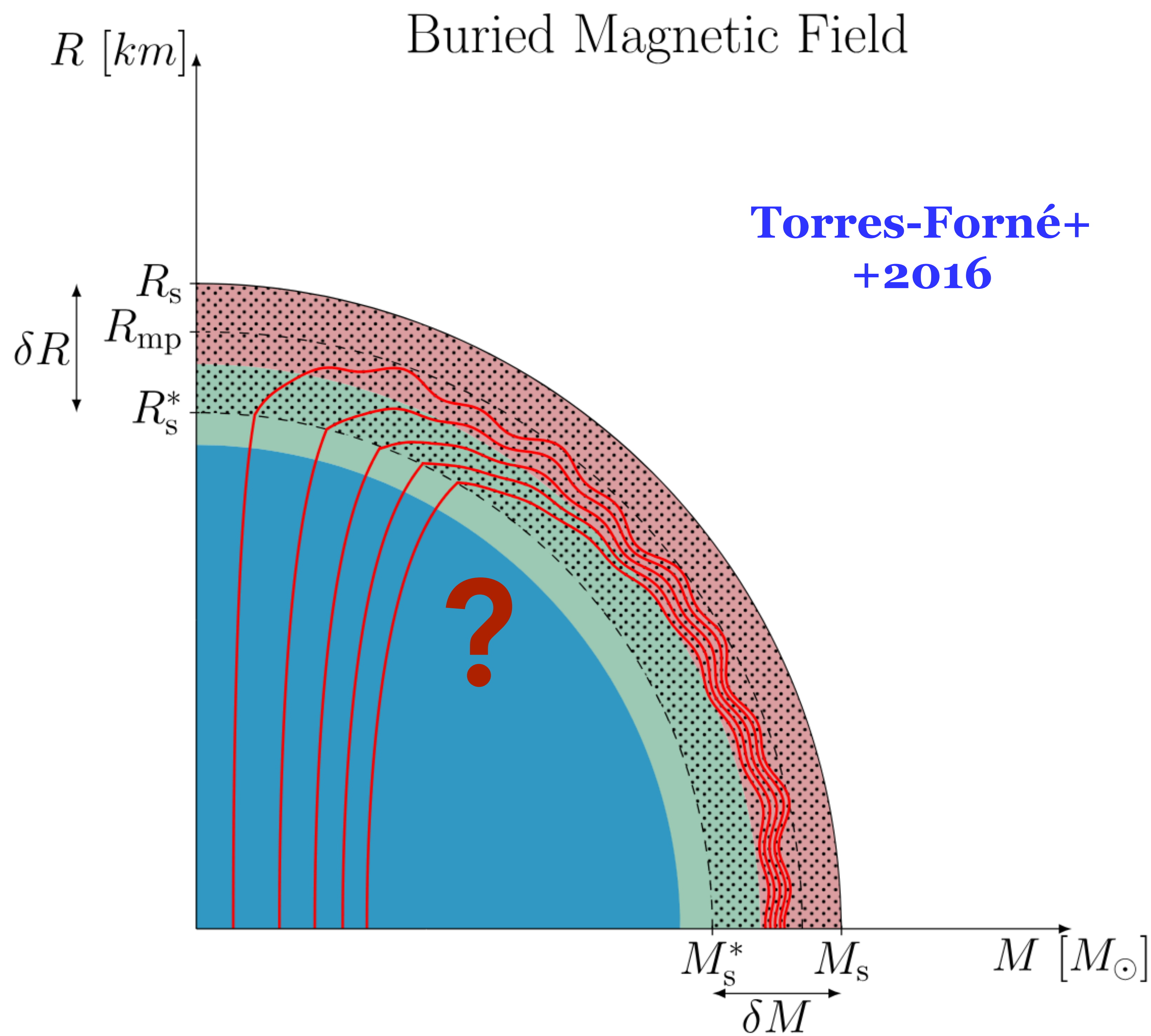

- Could also have current-like quadrupoles from unstable r-modes!

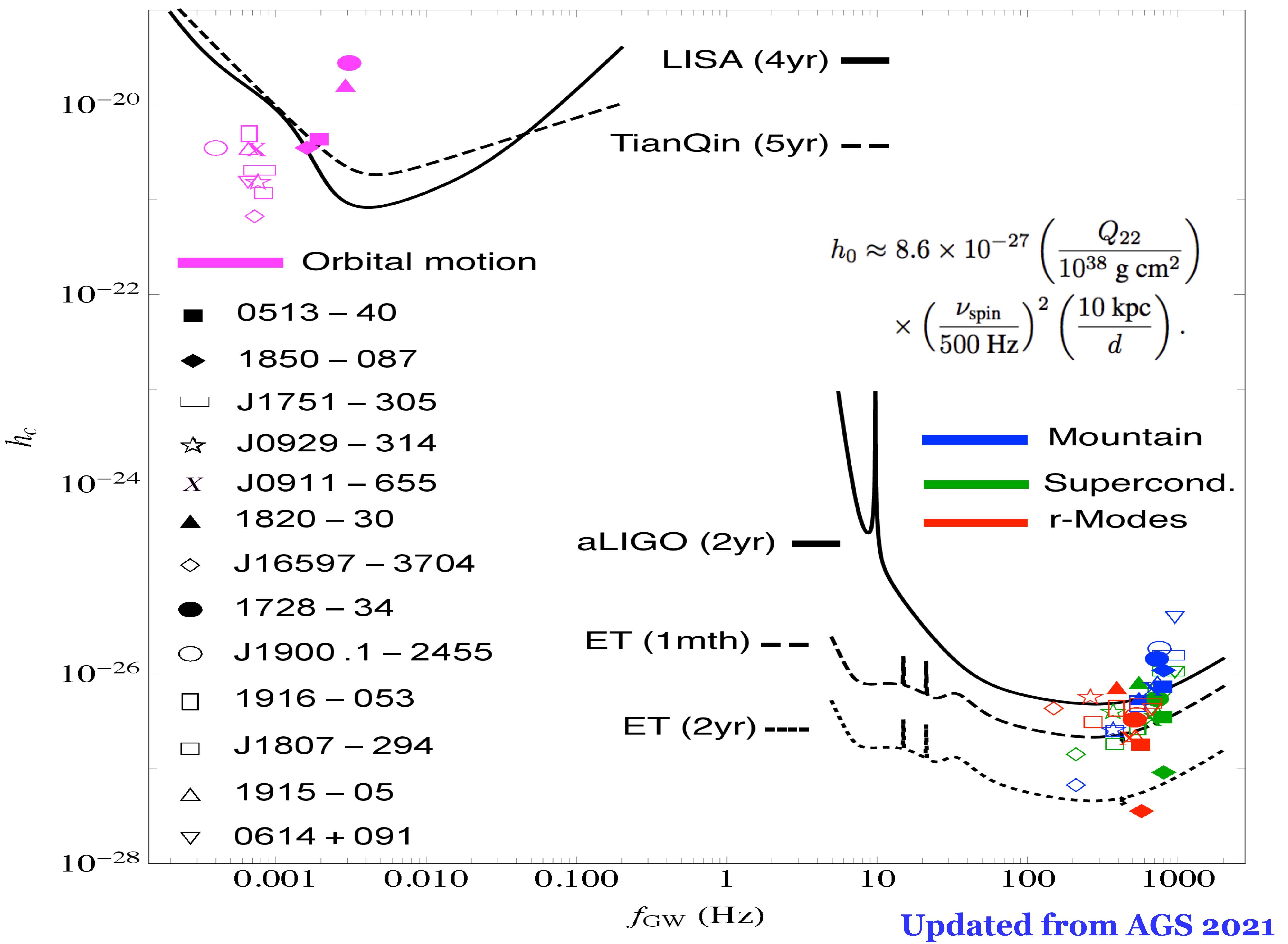

LISA (4yr)
TianQin (5yr)
Orbital motion
0513 − 40
1850 − 087
J1751 − 305
J0929 − 314
J0911 − 655
1820 − 30
J16597 − 3704
1728 − 34
J1900.1 − 2455
1916 − 053
J1807 − 294
1915 − 05
0614 + 091
$h_0 \approx 8.6 \times 10^{-27} \left(\frac{Q_{22}}{10^{38}\ \mathrm{g\ cm^2}}\right) \times \left(\frac{\nu_{\rm spin}}{500\ \mathrm{Hz}}\right)^2 \left(\frac{10\ \mathrm{kpc}}{d}\right).$
Mountain
Supercond.
r-Modes
aLIGO (2yr)
ET (1mth)
ET (2yr)
h_c
10^{-20}
10^{-22}
10^{-24}
10^{-26}
10^{-28}
0.001
0.010
0.100
1
10
100
1000
$f_{\rm GW}$ (Hz)
Updated from AGS 2021

THROWING FUEL ON THE FIRE

- Especially interesting for sources that exhibit thermonuclear activity: apparent emitting area and peak flux achieved during photospheric bursts can be used to independently constrain the mass–radius relationship of the star (**van Paradijs 1979**).
- LISA: can give a ~4% estimate on the NS mass (**Tauris 2018**)
- Thermonuclear bursts: ~percent-level estimate on M-R relationship
- Combined with LIGO ~percent estimate on Q22: can get a strong constraint on M-R-B space!

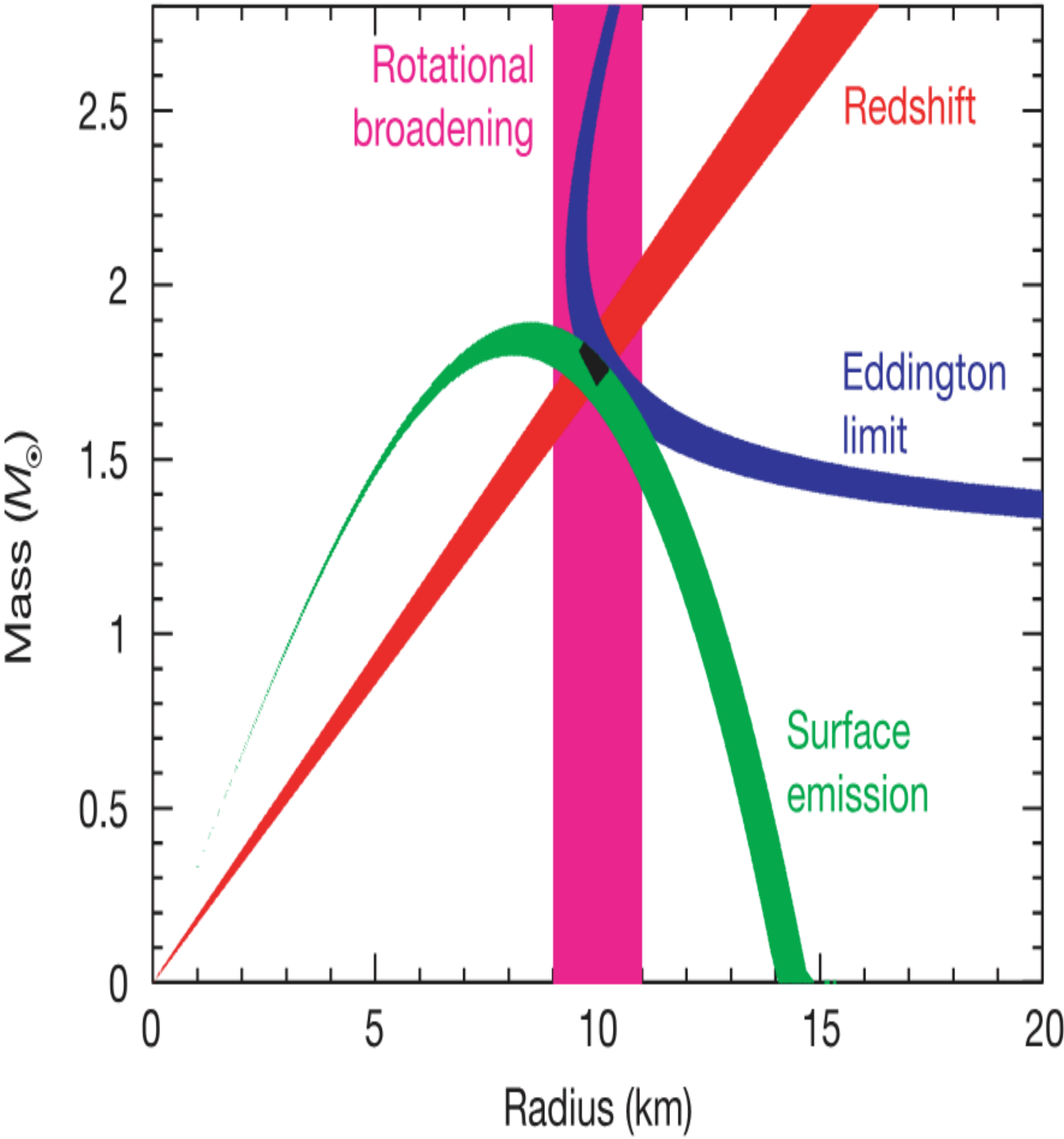

Özel 2006

THROWING FUEL ON THE FIRE

- Especially interesting for sources that exhibit thermonuclear activity: apparent emitting area and peak flux achieved during photospheric bursts can be used to independently constrain the mass–radius relationship of the star (**van Paradijs 1979**).

- LISA: can give a ~4% estimate on the NS mass (**Tauris 2018**)

- Thermonuclear bursts: ~percent-level estimate on M-R relationship

- Combined with LIGO ~percent estimate on Q22: can get a strong constraint on M-R-B space!

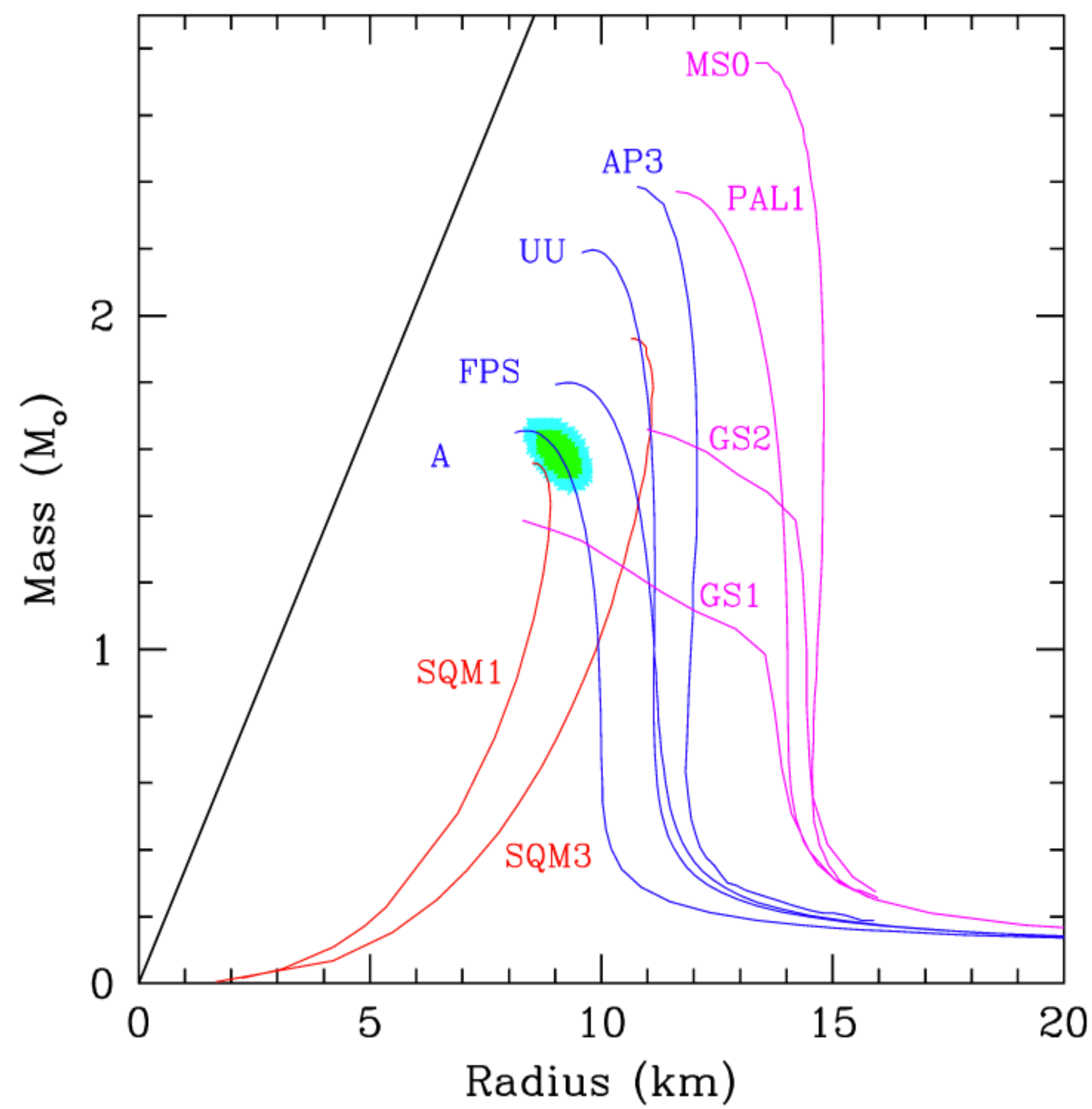

Güver et al. 2010

for 4U 1820-30

NS moment of inertia

$$I_{zz}\varepsilon = \left(\frac{2}{5}\right)^{1/2} (2\pi)^{-4/3} G^{2/3} \left(\frac{f_{\rm orb}^{1/3}}{f_{\rm spin}}\right)^2 \mathcal{M}^{5/3} \left(\frac{h_{\rm spin}}{h_{\rm orb}}\right)$$

ellipticity

LIGO

LISA

Tauris 2018

PUNCHLINE

- Purple: constraints on M-R from LISA
- Green: constraints on B-M-R from LIGO/ET
- Blue: constraints on M-R from bursts
- Red: anticipated overlap region

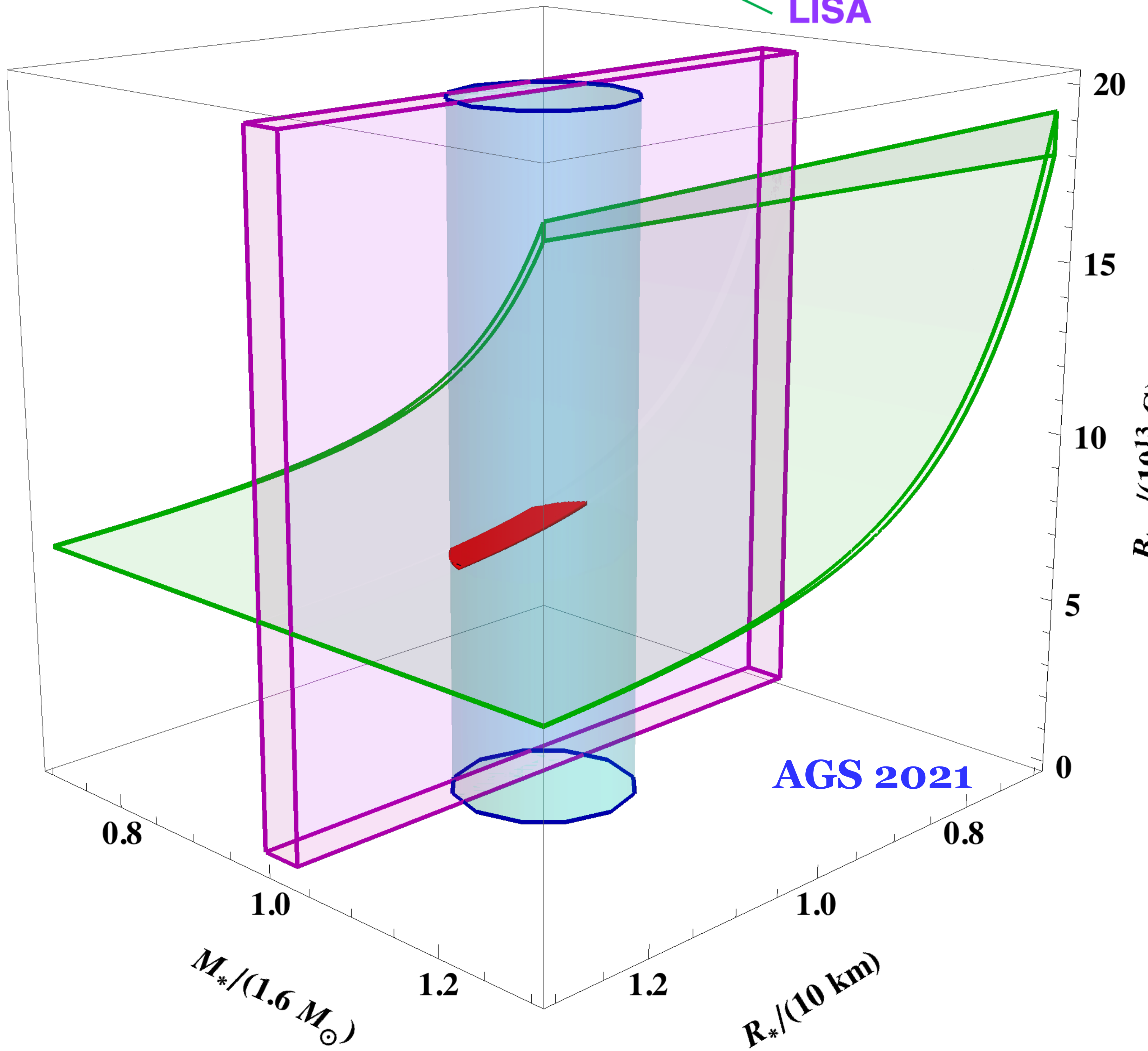

EXTRA EXTRA… READ ALL ABOUT IT

Table 1. Observed and derived properties related to the orbital and accretion dynamics of the UCXBs considered here. Companion masses $M_{\rm comp}$ are quoted either (in order of decreasing robustness) from observational upper-limits (asterisks), or the Rappaport et al. (1987) relation (4) (daggers). X-ray luminosities L_X are determined via the peak flux during outbursts in the case of sources exhibiting type I X-ray bursts.

Source	$P_{\rm orb}$ (s)	$M_{\rm comp}$ ($\times 10^{-2} M_\odot$)	L_X ($\times 10^{36}$ erg s^{-1})	d (kpc)
4U 1820-30[a]	685	$6.89^\dagger$	57	7.6
IGR J16597-3704[b]	2758	$1.71^\dagger$	6.5	9.1
4U 1728-34[c]	646	$7.30^\dagger$	5.0	5.1
HETE J1900.1-2455[d]	4995	8.5^*	3.7	4.3
XB 1916-053[e]	3005	10.1^*	6.6	8.4
XTE J1807-294[f]	2404	2.2^*	$\lesssim 13$	~ 8
4U 1915-05[g]	3027	$\sim 10^*$	~ 6	9.3
4U 0614+091[h]	3060	$1.54^\dagger$	3.4	3.2
4U 0513-40[i]	1020	$4.63^\dagger$	7.4	12
4U 1850-087[j]	1236	$3.82^\dagger$	1.7	8.2
XTE J1751-305[k]	2545	3.5^*	< 18.3	> 7
XTE J0929-314[l]	2615	$\sim 3^*$	< 13	$\gtrsim 7.4$

[a] Güver et al. (2010); Revnivtsev et al. (2011); Chen, Liu, & Wang (2020). [b] Sanna et al. (2018). [c] Galloway et al. (2010); Egron et al. (2011) [though cf. Vincentelli et al. (2020)]. [d] Falanga et al. (2007); Elebert et al. (2008). [e] Sometimes called 4U 1916-05; Church et al. (1997); Iaria et al. (2020). [f] Falanga et al. (2005); Riggio et al. (2008). [g] Grindlay et al. (1988); Zhang et al. (2014). [h] Sometimes called H 0614+091; Revnivtsev et al. (2011); Sazonov et al. (2020). [i] Revnivtsev et al. (2011); Chen, Liu, & Wang (2020). [j] Homer et al. (1996); Revnivtsev et al. (2011). [k] Markwardt et al. (2002); Gierliński & Poutanen (2005); Riggio et al. (2011). [l] Galloway et al. (2002); Marino et al. (2017).

Table 2. Observed and derived properties related to the NSs within the UCXBs considered in Tab. 1. Spin frequencies, listed in the second column, are deduced from (in order of decreasing robustness): pulsar timing (asterisks), type I X-ray burst tracking (daggers), and QPO frequency differentials (hashes). Surface magnetic field strength maxima $B_\star^{\max}$ are estimated from expression (6). For 4U 0513-40 and 4U 1850-087, where spin frequencies are unavailable, we instead assume $B_\star^{\max} = 10^{8.5}$ G and estimate $\nu_{\rm spin}$ from (6).

Source	$\nu_{\rm spin}$ (Hz)	$B_\star^{\max}$ ($\times 10^8$ G)	$M_\star$ ($M_\odot$)	$R_\star$ (km)
4U 1820-30[a]	$275^{\#}$	17.1	~ 1.58	~ 9.1
IGR J16597-3704[b]	105.2^{*}	14.0	(1.6)	(10)
4U 1728-34[c]	$363^{\dagger,\#}$	3.21	$\gtrsim 1.61$	$\gtrsim 9.6$
HETE J1900.1-2455[d]	377.3^{*}	2.38	(1.6)	(10)
XB 1916-053[e]	$270^{\dagger}$	5.22	$\lesssim 2.2$	(10)
XTE J1807-294[f]	190.6^{*}	16.5	$\gtrsim 1.67$	$\gtrsim 8.2$
4U 1915-05[g]	$366^{\#}$	3.14	(1.6)	(10)
4U 0614+091[h]	$477^{\dagger}$	1.74	$\lesssim 1.6$	(10)
4U 0513-40[i]	($\gtrsim 398$)	(3.16)	(1.6)	(10)
4U 1850-087[j]	(403)	(3.16)	$\gtrsim 1.23$	$\gtrsim 7.16$
XTE J1751-305[k]	435.3^{*}	4.48	(1.6)	(10)
XTE J0929-314[l]	185.1^{*}	10.3	(1.6)	(10)

[a] White & Zhang (1997); Güver et al. (2010). [b] Sanna et al. (2018). [c] Strohmayer, Zhang, & Swank (1997); Shaposhnikov, Titarchuk, & Haberl (2003). [d] Watts et al. (2009). [e] Galloway et al. (2001); Iaria et al. (2015). [f] Riggio et al. (2008); High-mass or large-radius stars preferred (Leahy, Morsink, & Chou 2011). [g] Ziólkowski (1999). [h] Klähn et al. (2006); Sazonov et al. (2020) [though cf. Strohmayer, Markwardt, & Kuulkers (2008) for a slightly different spin-frequency estimate]. [i] Difficult to measure mass or radius (Güver, Psaltis, & Özel 2012). Thermonuclear bursts detected at ≈ 1.38 kHz (Bilous & Watts 2019), consistent with rapid rotation. [j] Ray et al. (2004), assuming a strange star based on resonance absorption features. [k] Markwardt et al. (2002); estimates exist for $M_\star$ and $R_\star$ if the 2002 X-ray outburst is attributable to an r-mode, but considered unlikely by Andersson, Jones, & Ho (2014). [l] Galloway et al. (2002).

MASS QUADRUPOLES

- Many primaries within UCXBs do not have accurate measurements of their spin frequency *derivatives*, and thus it is hard to know how much they may be spinning down; but could be **large**!
- Three promising channels for generating a substantial quadrupole moment: mountains and superconducting toroidal fields for mass-type
- Mass type: twice the spin frequency; current-type: inertial mode frequency

$$h_0 \approx 8.6 \times 10^{-27} \left(\frac{Q_{22}}{10^{38}\ \mathrm{g\ cm^2}} \right) \times \left(\frac{\nu_{\mathrm{spin}}}{500\ \mathrm{Hz}} \right)^2 \left(\frac{10\ \mathrm{kpc}}{d} \right).$$

"Magnetic Mountain":

$$Q_{22} = A(M_\star, R_\star, \mu_i, \dot{M}, M_a) \times 10^{38}\ \mathrm{g\ cm^2},$$

(see, e.g., Suvorov+Melatos 2019)

Superconductor + hidden toroidal field:

$$Q_{22} \approx 1.88 \times 10^{38}\ \mathrm{g\ cm^2} \times \left(\frac{\lambda b B_{\star,\mathrm{max}}}{10^{14}\ \mathrm{G}} \right) \left(\frac{H_{c1}}{10^{15}\ \mathrm{G}} \right) \times \left(\frac{I_0}{10^{45}\ \mathrm{g\ cm^2}} \right) \left(\frac{1.6 M_\odot}{M_\star} \right)^2 \left(\frac{R_\star}{10^6\ \mathrm{cm}} \right)^4,$$

(see, e.g., Cutler 2002)